

# ROBUST CONTROLLER FOR THE VIBRATION SUPPRESSION OF AN ACTIVE PIEZOELECTRIC BEAM

Tamara Nestorović\*, Atta Oveisi†

Ruhr-Universität Bochum

Mechanik adaptiver Systeme, Universitätsstraße 150, 44801 Bochum, Germany

\*tamara.nestorovic@rub.de, †atta.oveisi@rub.de

**Key words:** Smart piezoelectric beam, Vibration suppression, Robust control.

**Summary:** *Design and control of smart structures, which can perform optimally despite different environmental influences represents an important research challenge. Very often the optimality performance is influenced by the lack of robustness of mechanical systems due to unmodeled dynamics and external influences. In this paper we tackle the problem of a robust controller design for the vibration suppression of a smart beam with integrated active piezoelectric ceramic material in order to reach the desired robust stability. For this purpose a multi-objective robust control strategy is proposed for vibration suppression of a clamped-free smart beam with piezoelectric actuator and a laser vibrometer sensor in a Linear Matrix Inequality (LMI) framework which is capable of handling weighted exogenous input signals and provides desired pole placement and robust performance at the same time. A Finite Element Analysis (FEA) based reduced order modal system is considered as the nominal model and the remaining modes are left as the multiplicative unstructured uncertainty. A robust controller with a regional pole placement constraint is designed based on the augmented plant composed of the nominal model and its accompanied uncertainty by solving a convex optimization problem. For designed control system the robustness of the uncertain closed-loop model and the effect of performance index weights on the system output are investigated both in simulation and experiment. As critical case, the periodic excitation with the frequency corresponding to the first bending eigenfrequency of the beam is investigated. The implementation of the robust controller results in a considerable suppression of the velocity magnitude measured by the vibrometer at the tip of the beam.*

## 1 INTRODUCTION

Adaptive structures play a crucial role in challenging areas of applied science where high quality performance is required in the presence of changing environment. Introduction of multifunctional material based transducers together with highly integrated control represent the basic concept of smart structures. The evolution of mechanical and aeronautical structures comes out with an increasing demand on the structures to be lighter and at the same time controllable. Overcoming some lacks of those systems, especially their sensitivity to unwanted disturbances has attracted many researchers over the past couple of decades in fields of structural vibration analysis, damage detection, vibration control and noise control.

Among various suggested methods of dynamics control, the use of active control

techniques in vibration suppression of light weight structures has been proven as advantageous over passive methods, especially if additional masses of stiffeners or dampers should be avoided. Active techniques are also more suitable in cases where the disturbance to be cancelled or the properties of the controlled system vary with time [1].

Piezoelectric actuators are widely employed in many practical applications due to their capability of coupling strain and electric field. In order to control structural vibrations, piezoelectric actuators can be easily bonded on the vibrating structures.

Very often development of appropriate control techniques requires reliable dynamic models. In [2] Benjeddou presents an overview of the development in the field of the finite element (FE) based modeling of active structures, which has become a standard numeric modeling procedure to capture structural dynamics properties. An overview of the various types of controller design methods is presented in [3]. Some particular controllers are related to velocity feedback control [4], high gain feedback regulator [5], linear quadratic regulator (LQR) [6] or  $H_\infty$  control [7]. Some experimental work has been shown in [8].

The authors of this paper have contributed to the piezoelectric coupled-field problems by implementing their own developed FE based tools into commercially available software packages [9], by identifying models based on experimental measurements [10], dealing with control techniques for adaptive structures [11, 12] etc.

In this work, an accurate model of a piezo-laminated cantilever beam is derived based on the finite element modal analysis, which is performed in order to calculate the eigenfrequencies and mode shapes of the coupled electro-elastic system. The derived formulation provides the state space model relating the actuator voltage to sensor voltage. The obtained model is capable of offering a finite order model that shall be considered as nominal system and remaining high order states are left as a multiplicative unstructured uncertainty of modeling. Then, a multi-objective robust controller is designed based on the augmented plant composed of the nominal model and its accompanied uncertainty. In addition, a regional pole placement constraint is included within the Linear Matrix Inequality (LMI) framework to improve closed-loop transient performance. The robust controller is implemented to a clamped active beam with piezoelectric patches and finally the performance of the closed loop system is evaluated experimentally.

## 2 MODEL DEVELOPMENT

A general modeling procedure is introduced, which is based on the FE approach to modeling of the coupled electro-mechanical behavior of smart structures. This approach is applicable to various types of structural geometries, depending on the developed method for defining the coupled problem. In this particular case, the bending vibrations of a cantilever beam are considered, and therefore the torsional modes are not considered in the controller design. The modeling procedure assumes derivation of a set of ordinary differential equations resulting from the FE analysis, which are subsequently converted into a linear time invariant (LTI) system since it is a convenient model for the work in the computer aided control system design.

It is assumed that the displacements are small enough so that the dynamics of the system remains in linear piezo-elasticity. The finite element method provides the dynamic equation of motion in matrix representation as

$$M\ddot{q} + C\dot{q} + Kq = F, \quad (1)$$

With  $M$ ,  $C$  and  $K$  being the mass, damping and stiffness matrices. Also,  $q$  represents the

nodal states of displacement and electric potential

$$q = [u_1^T \quad \phi_1 \quad \cdots \quad u_n^T \quad \phi_n]^T. \quad (2)$$

$F$  represents the applied external forces, where the external input disturbance is assumed to affect the system from the same channel as the control input. External forces are therefore assumed in the following form of the vector of control forces:

$$F = Bu(t), \quad (3)$$

where matrix  $B$  describes the position of the generalized control effort in the finite element structure, with  $u$  consisting of all modal inputs. For the control design purposes the measurement signal is represented in terms of system states and plant inputs as

$$y = C_{0q}q + C_{0v}\dot{q}, \quad (4)$$

in which  $C_{0q}$  and  $C_{0v}$  are the output displacement and output velocity matrices, respectively and they are calculated using the FE procedure and choosing the appropriate sensor location. By applying the conventional harmonic solution of  $q = \phi e^{i\omega t}$  one can easily find the natural frequencies  $\omega_j$  and the mode shapes  $\phi_j$  ( $j=1,2,\dots,n$ ) solving the determinant of homogenous system of algebraic equations. The solution can be represented in matrix form as

$$\Omega = \begin{bmatrix} \omega_1 & 0 & \cdots & 0 \\ 0 & \omega_2 & \cdots & 0 \\ \vdots & \vdots & \ddots & \vdots \\ 0 & 0 & \cdots & \omega_n \end{bmatrix}, \quad \Phi = \begin{bmatrix} \phi_{11} & \phi_{21} & \cdots & \phi_{n1} \\ \phi_{12} & \phi_{22} & \cdots & \phi_{n2} \\ \vdots & \vdots & \ddots & \vdots \\ \phi_{1n} & \phi_{2n} & \cdots & \phi_{nn} \end{bmatrix} = [\phi_1 \quad \phi_2 \quad \phi_3 \quad \phi_4]. \quad (5)$$

The nodal model representation (1) can be transformed to modal coordinates by applying the following conversion

$$q = \Phi q_m, \quad (6)$$

where  $q_m$  is the vector of generalized modal displacement. Using the symmetricity of the mass and stiffness matrices, the modally transformed matrices are obtained as [13]

$$\Phi^T M \Phi = M_m = \text{diag}(m_j), \quad \Phi^T K \Phi = K_m = \text{diag}(m_j \omega_j^2). \quad (7)$$

Using the orthogonality properties and under assumption of proportional damping (8), a decoupled system of differential equations can be obtained, which enables numerical solution of the problem. This is the part of a standard FE based modelling procedure.

$$C = \alpha M + \beta K. \quad (8)$$

Selecting the state vector in the form  $x = [\Omega q_m \quad \dot{q}_m]^T$  the state space model will be

$$\dot{x} = Ax + Bu, \quad y = Cx + Du \quad (9)$$

where

$$A = \begin{bmatrix} 0 & \Omega \\ -\Omega & 2Z\Omega \end{bmatrix}, \quad B = \begin{bmatrix} 0 \\ B_m \end{bmatrix}, \quad C = [C_{mq} \quad C_{mv}], \quad D = 0, \quad (10)$$

while  $\Omega^2 = M_m^{-1}K_m$  and  $Z = \text{diag}(\zeta_j)$  with  $\zeta_j$  being the damping ratio of the  $j^{\text{th}}$  mode and  $B_m = \Phi^T B$ ,  $C_{mq} = C_{0q} \Phi$ ,  $C_{mv} = C_{0v} \Phi$ .

### 3 CONTROLLER DESIGN

Controller which should be implemented for the vibration suppression is a multi-objective robust controller. It is designed based on the augmented plant composed of the nominal model and its accompanied uncertainty. In addition, a regional pole placement constraint is included within the LMI framework to improve closed-loop transient performance. The closed-loop system with considered multiplicative uncertainty is shown in Fig. 1,

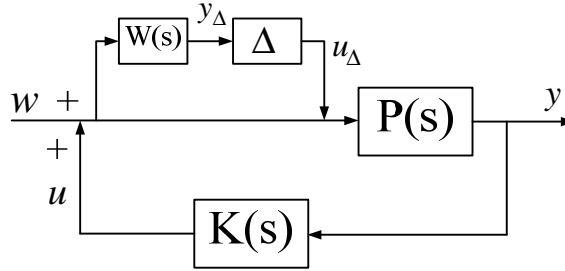


Figure 1: Closed-loop system with multiplicative uncertainty.

where  $P(s)$  is the nominal plant,  $K(s)$  is desired controller,  $\Delta$  is a stable transfer function, where  $\|\Delta\|_\infty < 1$  and  $W(s)$  is the weighting function for multiplicative uncertainty, that satisfies following equation:

$$\frac{P_{real}(s)}{P(s)} - 1 < W(s) \quad (11)$$

where  $P_{real}(s)$  is the transfer function of the real system, by considering all or some of the higher modes. Note that, reduction of the order of the nominal plant will hold the designed controller's order in a lower value, but the price will be reduced performance. For robust stability, one should have  $\|T_{y_\Delta u_\Delta}\|_\infty < 1$ , where  $T_{y_\Delta u_\Delta}$  is the transfer function from  $u_\Delta$  to  $y_\Delta$  when  $\Delta$  is removed [14]. However, to handle the stochastic aspects such as measurement noise and random disturbance, despite the robust  $H_\infty$ , only the  $H_2$  performance is functional. And finally, for appropriate disturbance rejection and control effort the conventional optimization problem is to minimize  $\|y^T Q y + u^T R u\|_\infty$ , where  $Q$  and  $R$  are two weighting functions that indicate the relative importance of disturbance rejection and control effort, respectively. For minimizing the performance index  $\|y^T Q y + u^T R u\|_\infty$ , we should minimize  $\|T_{[y \ u]^T w}\|_2$  instead, where  $w$  is a bounded  $H_2$  norm exogenous disturbance. This will be addressed later. The transient response of a linear system is well known to be related to the locations of its closed-loop poles. This will be the next issue that has to be addressed.

Since  $T_{y_\Delta u_\Delta}$  is equivalent to  $T_{uw} W(s)$  [15], the above system can be represented as shown in Fig. 2 with all of the constraints that have to be satisfied in order to reach the predefined  $H_2 / H_\infty$  performance and optimal control effort.

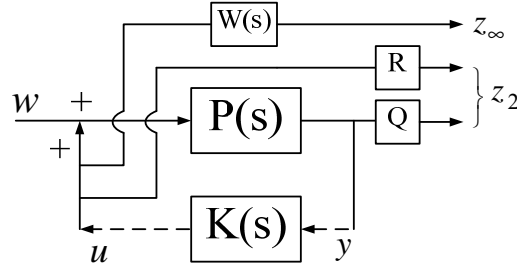


Figure 2: Desired input and outputs of augmented plant.

Now assume that a state space representation of the open-loop system in Fig. 2 (by ignoring  $K(s)$ ) is

$$\begin{cases} \dot{x} = Ax + B_1 w + B_2 u \\ z_\infty = C_\infty x + D_{\infty 1} w + D_{\infty 2} u \\ z_2 = C_2 x + D_{21} w + D_{22} u \\ y = C_y x + D_{y1} w \end{cases} \quad (12)$$

where  $u$  and  $w$  are control input and disturbance, respectively. Our objective is to design a dynamic output-feedback controller with the state space realization

$$\begin{cases} \dot{\zeta} = A_\kappa \zeta + B_\kappa y \\ u = C_\kappa \zeta + D_\kappa y \end{cases} \quad (13)$$

where  $\zeta$  is the state variable of the controller. Therefore, the corresponding closed-loop system containing the performance and robustness channels will be

$$\begin{cases} \dot{x}_{cl} = A_{cl} x_{cl} + B_{cl} w \\ z_\infty = C_{cl1} x_{cl} + D_{cl1} w \\ z_2 = C_{cl2} x_{cl} + D_{cl1} w \end{cases} \quad (14)$$

Our three design objectives can be expressed as follows.

**$H_\infty$  performance:** the closed-loop RMS gain from  $w$  to  $z$  does not exceed  $\gamma$  if and only if there exists a symmetric matrix  $X_\infty$  such that [16]

$$\begin{pmatrix} A_{cl} X_\infty + X_\infty A_{cl}^T & B_{cl} & X_\infty C_{cl1}^T \\ B_{cl}^T & -I & D_{cl1}^T \\ C_{cl1} X_\infty & D_{cl1} & -\gamma^2 I \end{pmatrix} < 0, \quad X_\infty > 0 \quad (15)$$

This LMI constraint is used to minimize  $\|T_{z_\infty w}\|_\infty$  (closed-loop  $H_\infty$  gain from disturbance to  $z_\infty$  output channel).

**$H_2$  performance:** the  $H_2$  norm of the closed-loop transfer function from  $w$  to  $z_2$  does not exceed  $v$  if and only if  $D_{cl2} = 0$  and there exist two symmetric matrices  $X_2$  and  $Q$  such that [17]:

$$\begin{pmatrix} A_{cl} X_2 + X_2 A_{cl}^T & B_{cl} \\ B_{cl}^T & -I \end{pmatrix} < 0, \quad \begin{pmatrix} Q & C_{cl2} X_2 \\ X_2 C_{cl2}^T & X_2 \end{pmatrix} > 0, \quad \text{Trace}(Q) < v^2 \quad (16)$$

**Pole placement:** the closed-loop poles lie in the LMI region

$$D = \{z \in \mathbb{C} : L + Mz + M^T \bar{z} < 0\} \quad (17)$$

with  $L = L^T = \{\lambda_{ij}\}_{1 \leq i, j \leq m}$  and  $M = [\mu_{ij}]_{1 \leq i, j \leq m}$  if and only if there exists a symmetric matrix  $X_{pol}$  satisfying

$$\begin{aligned} & \left[ \lambda_{ij} X_{pol} + \mu_{ij} A_{cl} X_{pol} + \mu_{ji} X_{pol} A_{cl}^T \right]_{1 \leq i, j \leq m} < 0 \\ & X_{pol} > 0 \end{aligned} \quad (18)$$

For tractability in the LMI framework, we must seek a single Lyapunov matrix

$$X := X_\infty = X_2 = X_{pol} \quad (19)$$

that enforces all three sets of constraints. Factorizing  $X$  as

$$X = X_1 X_2^{-1}, X_1 := \begin{pmatrix} R & I \\ M^T & 0 \end{pmatrix}, X_2 := \begin{pmatrix} 0 & S \\ I & N^T \end{pmatrix} \quad (20)$$

and, introducing the change of controller variables [18]:

$$\begin{cases} B_K := NB_K + SB_2 D_K \\ C_K := C_K M^T + D_K C_y R \\ A_K = NA_K M^T + NB_K C_y R + SB_2 C_K M^T + S(A + B_2 D_K C_y)R \end{cases} \quad (21)$$

the inequality constraints on  $X$  are readily turned into LMI constraints in the variables  $R, S, Q, A_k, B_k, C_k$  and  $D_k$  [16, 19]. This leads to the suboptimal LMI formulation of our multi-objective synthesis problem, which is defined as:

Minimize  $\alpha \cdot \gamma^2 + \beta \cdot \text{trace}(Q)$  over variables  $R, S, Q, A_k, B_k, C_k$  and  $D_k$  and  $\gamma^2$  satisfying [20]:

$$\begin{aligned} & \begin{pmatrix} AR + RA^T + B_2 C_K + C_K^T B_2^T & A_K^T + A + B_2 D_K C_y & B_1 + B_2 D_K D_{y1} & H \\ H & A^T S + SA + B_K C_y + C_y^T B_K^T & SB_1 + B_K D_{y1} & H \\ H & H & -I & H \\ C_\infty R + D_{\infty 2} C_K & C_\infty + D_{\infty 2} D_K C_y & D_{\infty 1} + D_{\infty 2} D_K D_{y1} & -\gamma^2 I \end{pmatrix} & (22) \\ & \begin{pmatrix} Q & C_2 R + D_{22} C_K & C_2 + D_{22} D_K C_y \\ H & R & I \\ H & I & S \end{pmatrix} > 0 \\ & \left[ \lambda_{ij} \begin{pmatrix} R & I \\ I & S \end{pmatrix} + \mu_{ij} \begin{pmatrix} AR + B_2 C_K & A + B_2 D_K C_y \\ A_K & SA + B_K C_y \end{pmatrix} + \mu_{ij} \begin{pmatrix} RA^T + C_K^T B_2^T & A_K^T \\ (A + B_2 D_K C_y)^T & A^T S + C_y^T B_K^T \end{pmatrix} \right]_{1 \leq i, j} \\ & \text{Trace}(Q) < v_0^2 \\ & \gamma^2 < \gamma_0^2 \\ & D_{21} + D_{22} D_K D_{y1} = 0 \end{aligned}$$

Given optimal solutions  $\gamma^*$ ,  $Q^*$  of this LMI problem, the closed-loop  $H_\infty$  and  $H_2$  performances are bounded by

$$\|T_\infty\|_\infty \leq \gamma^*, \quad \|T_2\|_2 \leq \sqrt{\text{trace}(Q^*)} \quad (23)$$

#### 4 EXPERIMENTAL SETUP AND CONTROLLER IMPLEMENTATION

The structure of the experimental smart beam is presented in Fig. 3. The piezo-laminated beam consists of a cantilever aluminum beam with Young's modulus 70 GPa and density 2.7 g/cm<sup>3</sup>. In addition since the ultimate goal is to suppress the vibration, two piezoelectric actuators (DuraAct™ P-876.A15) are attached to the beam at the same side (see Fig. 3).

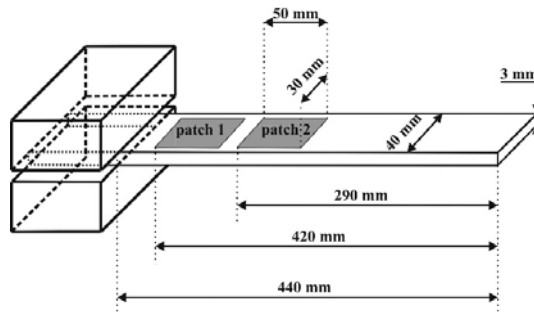


Figure 3: Geometry of the smart beam.

The feedback channel entails the measurement signal namely, the signal measured by a scanning digital laser Doppler vibrometer VH-1000-D. This will provide the measurement of the velocity of the lateral vibration at a point, close to the free end of the beam. Schematic configuration of the closed-loop vibration control system is presented in Fig. 4.

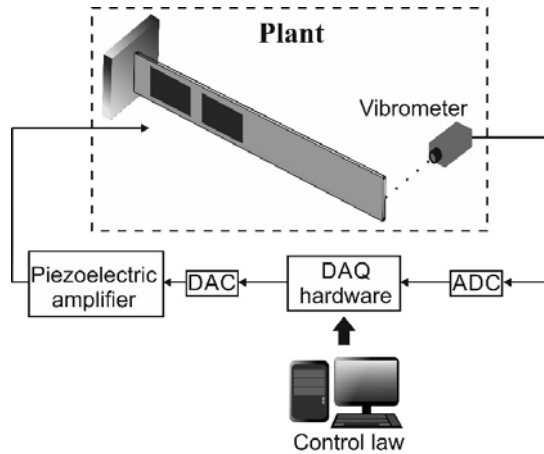


Figure 4: Sketch of experimental setup.

It is worthwhile mentioning that the plant has two inputs: the control input which acts on the actuator piezo-patch and the disturbance signal which excites the system through the disturbance channel. Moreover, the only output of the system is recorded using the previously mentioned vibrometer.

For implementing the controller in real time, a dSPACE digital data acquisition and real-time control system with DS1005 digital signal process board is used. Connection of the

digital data acquisition system with the actuators and the computer is provided by an ADC Board DS2004 (Analog to Digital Converter) and a DAC Board DS2102 (Digital to Analog Converter). To increase the working range of the DAC boards the control input is amplified (PI E-500). The control law, for the active vibration control of the smart beam, is then implemented on MATLAB platform. Finally, the control system is downloaded to the dSPACE digital data acquisition and real-time control system.

The vibration damping quality of the proposed method will be subsequently shown both in simulation and experiment. The model of the structure for control design purposes is obtained based on the method described in Section 2. Since the actuator placement plays an important role in vibration control performance the optimal placement of the actuator is addressed based on the mixed  $H_2 / H_\infty$  method as described in [21].

One should notice that the torsional modes are not considered in controller design because they are not relevant for the bending vibration. It should be mentioned that due to the previous research the dominant mode shape of the flexible beam is the first mode shape [17].

First two shape numbers of the clamped beam are considered as nominal model and higher order modes remain as unstructured uncertainty. In addition, a weighting function for multiplicative unstructured uncertainty that satisfies  $\frac{P_{real}(s)}{P(s)} = W_{unc}(s) + 1$  is considered, with

$P_{real}(s)$ ,  $P(s)$  and  $W_{unc}(s)$  being the full order transfer function of the system, nominal transfer function and frequency based appropriate weighting function representing the unstructured uncertainty, respectively. Fig. 5 shows the weighting functions that are considered for modeling unstructured uncertainty, disturbance and  $H_2 / H_\infty$  performance.

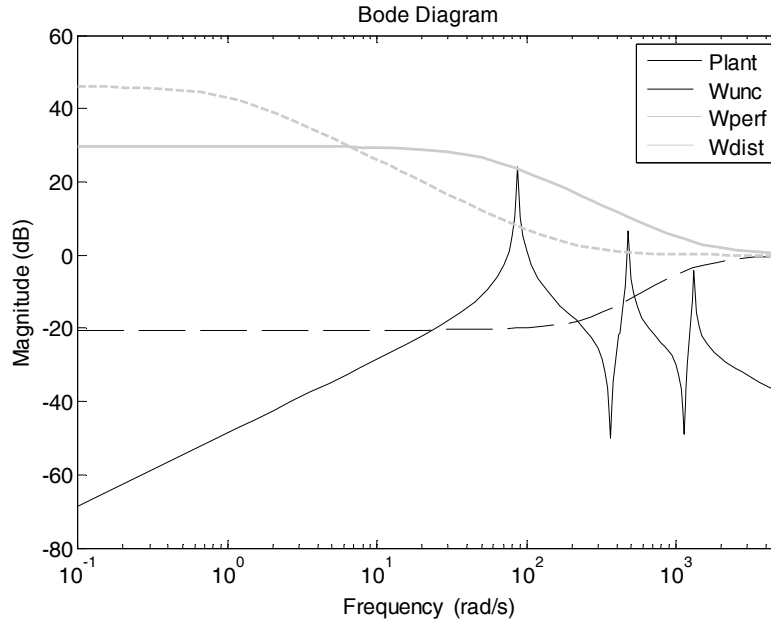


Figure 5: The relation of weighting function to real system.

The design of desired controller is carried out by solving convex optimization problem that is formulated in Eq. (22). For obtaining an appropriate  $H_\infty$  performance, the magnitude of  $|\gamma|$  should be under unit and for increasing the performance one should minimize  $H_2$  norm

from exogenous disturbance to performance index. The relative magnitudes of  $Q$  and  $R$  determine the relative importance of disturbance rejection (vibration suppression) to control effort (actuator saturation). To improve transient performance, as mentioned before, one shall resort to an additional regional pole placement constraint in order to achieve a better closed-loop damping across the uncertainty range. This places the closed-loop poles into a suitable sub-region of the left-half plane that can be expressed as an additional LMI constraint. A typical example of LMI region that is commonly treated in multi-objective synthesis that guarantees  $H_2$  stability is the conic sector centered at the origin and with inner angle  $2\theta = 2\cos^{-1}(\zeta)$  [16]. In this work, the closed-loop damping coefficient is assumed to be  $\zeta = 0.1$ .

The controller is designed by setting  $Q = 10$ . Comparison of the impulse response of the closed-loop system with this controller and the impulse response of the open-loop system (Fig. 6) shows the performance of the controller in suppressing the vibration.

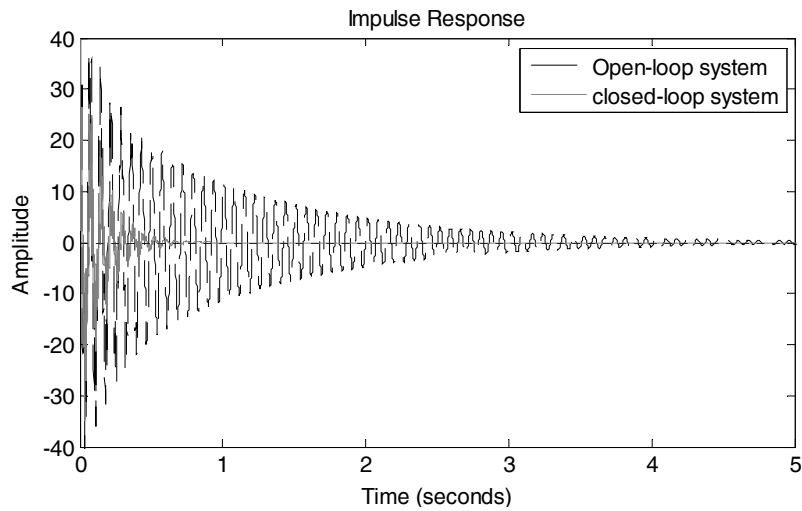


Figure 6: Impulse response of the open-loop and closed-loop system.

Actuator voltage of this controller during the impulse response is plotted in Fig. 7.

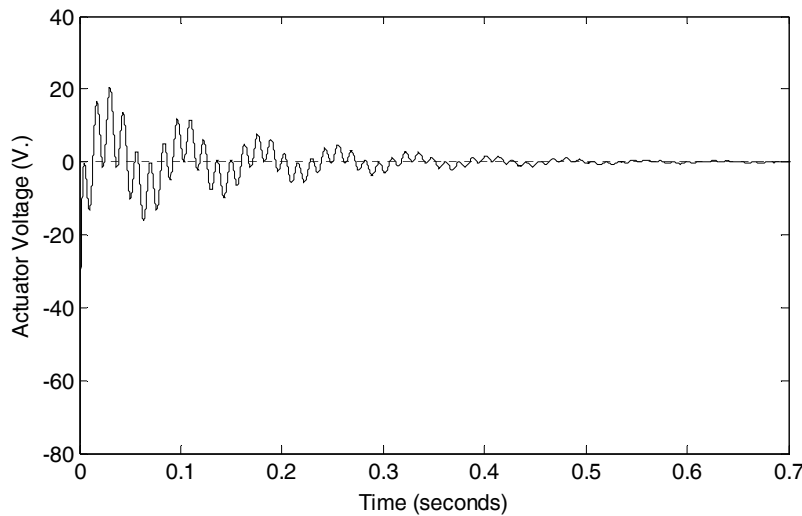


Figure 7: Input control for impulse response of the closed-loop system.

In addition, comparison of frequency responses of the closed-loop and the open-loop system is shown in Fig. 8. This figure shows that the amplitude is reduced at the nominal model natural frequencies.

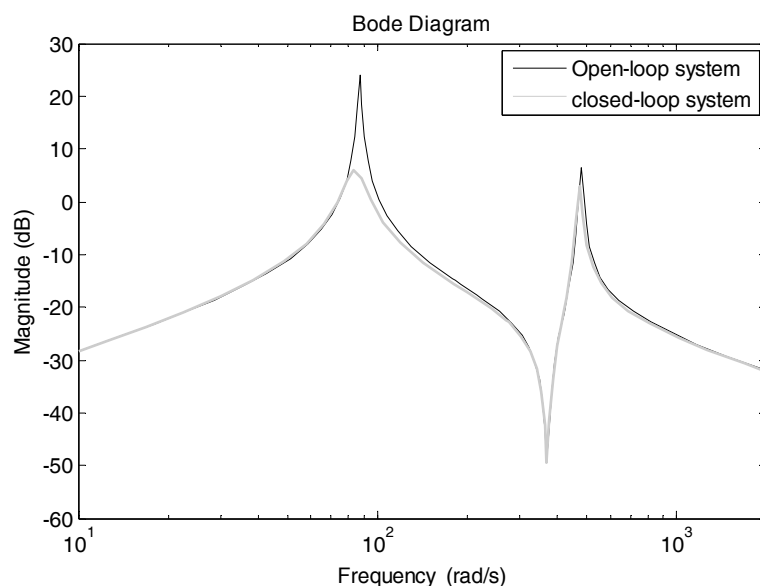


Figure 8: Bode diagram of closed-loop system and open-loop system.

For investigation of the robust performance of the uncertain closed-loop system with the designed controller by structured singular value analysis, Fig. 9 is obtained. This plot shows upper/lower bounds of uncertain closed-loop structured singular values in frequency domain.

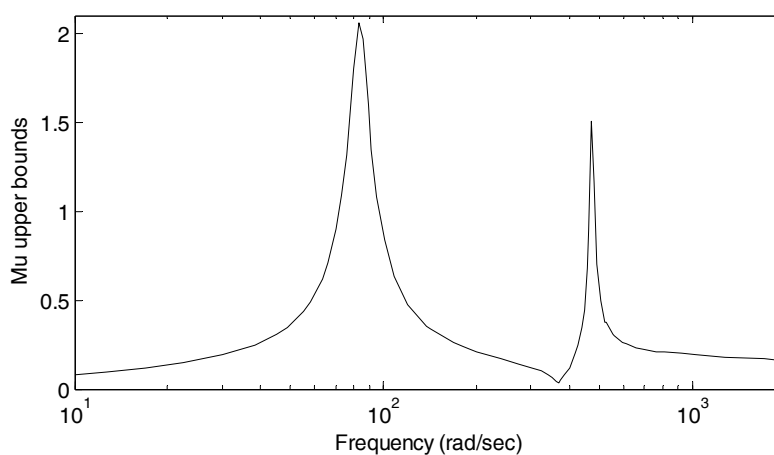


Figure 9:  $\mu$  bounds of uncertain closed-loop system.

The performance margin is the reciprocal of the structured singular value and if the magnitude of the structured singular value is under unit, in entire frequency range, the system has robust performance. Therefore, upper bounds from structured singular value become lower bounds on the performance margin and critical frequency associated with the upper bound of the structured singular value, here is  $\omega_{critical} = 87 rad / sec$ . In addition, the system can tolerate up to 557% of the modeled uncertainty without losing desired performance.

Through the experimental implementation of the control law on the smart structure the possibility of the successful vibration control performance was evaluated on the full order

system. The vibration amplitude suppression will be demonstrated under the harmonic excitation of the piezo-beam through the control channel and the results obtained using hardware in loop system with dSPACE RTI platform. Experimental excitation is considered to be harmonic  $F(t) = A\sin(2\pi f_j t)$ , with  $f_j$  being the first bending resonant frequency of the clamped piezo-beam. The closed-loop system is implemented on the real time data acquisition platform of the dSPACE with sampling frequency of 10 kHz. The predefined task of the controller is to guarantee the robust stability and performance in conjugation with real time vibration amplitude suppression in frequency ranges close to resonance eigenvalues. Therefore, investigations are carried out in time domain by means of the experimental setup shown in Fig. 10.

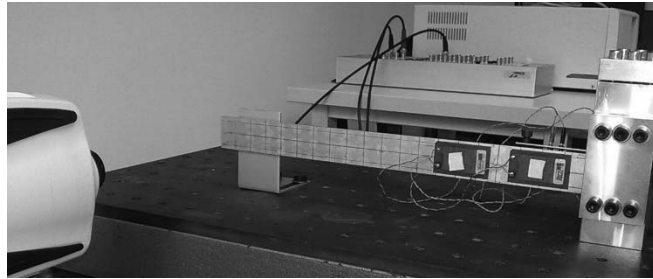


Figure 10: Experimental rig of the closed-loop system.

For the analysis in time domain the sinusoidal excitation signal is generated in Simulink and lead out through the dSPACE DAC. The frequency of the excitation is adjusted experimentally to reach the highest vibration amplitude representing the actual eigen-frequency. The response of the system for controlled and uncontrolled case is shown in Fig. 11 based on the measurement signal generated by Doppler vibrometer.

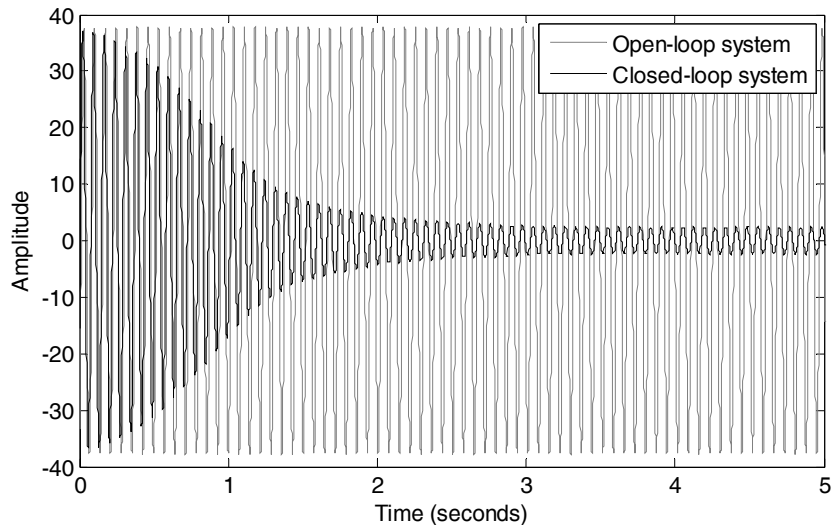


Figure 11: Experimental comparison of velocity response.

This diagram shows the velocity magnitudes of the beam measured by dSPACE ADC board. In addition the corresponding control effort generated for piezo-actuator patches by the dSPACE DAC board is shown in Fig. 12.

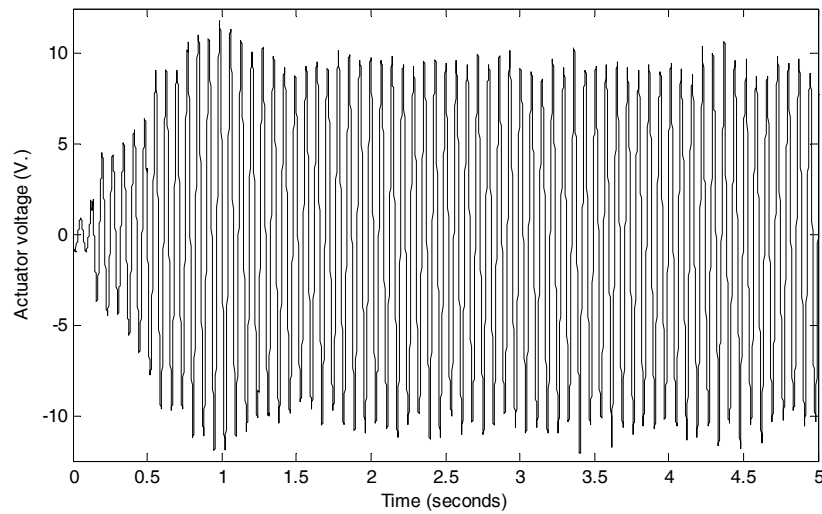


Figure 12: Control effort of the piezo-patch actuator.

The experimental results show the obvious performance of the robust control system in attenuating the vibration amplitude.

## 5 CONCLUSIONS

Vibration control of a clamped-free beam with piezoelectric actuator and vibrometer has been achieved using a multi-objective robust output feedback control strategy with regional pole placement constraints in an LMI framework, based on  $H_2/H_\infty$  weighting objective functions. The robustness of the closed loop smart beam with respect to external input disturbance increased to 557% of the modeled uncertainty. The regional pole placement constraints guaranteed the improvement of the transient response of the closed-loop system and the optimality of the control effort is achieved by satisfying the appropriate  $H_2$  LMI based performance index. All these constraints are presented in an LMI formulation, which is solvable in the MATLAB environment. Finally, the performance of the approach is proven to be effective and robust on the experimental set up where the higher order modes take effect in the dynamics of the smart beam.

## REFERENCES

- [1] Carra, S., Amabili, M., Ohayon, R., Hutin, P. M., 2008, Active vibration control of a thin rectangular plate in air or in contact with water in presence of tonal primary disturbance, *Aerospace Science and Technology*, 12 pp. 54-61
- [3] Benjeddou, A., 2000, Advances in piezoelectric finite element modeling of adaptive structural elements: a survey, *Computers & Structures*, 76(1-3) pp. 347-363
- [4] Gao, L., Lu, Q., Fei, F., Liu, L., Liu, Y., Leng, J., 2013, Active vibration control based on piezoelectric smart composite, *Smart Materials and Structures*, 22(12) 125032
- [5] Tavakolpour, A. R., Mailah, M., Mat Darus, I. Z., 2009, Active vibration control of a rectangular flexible plate structure using high gain feedback regulator, *International*

*Review of Mechanical Engineering*, 3(5) pp. 579-587

- [6] Narayanan S., Balamurugan V., 2003, Finite element modeling of piezolaminated smart structures for active vibration control with distributed sensors and actuators, *Journal of Sound and Vibration*, 262 pp. 529-562
- [7] Oveisi, A., Gudarzi, M., Mohammadi, M.M., Doosthoseini, A., 2013, Modeling, identification and active vibration control of a funnel-shaped structure used in MRI throat, *Journal of Vibroengineering*, 15(1) pp. 438-450
- [8] Qiua, Z., Wub, H., Zhanga, D., 2009, Experimental researches on sliding mode active vibration control of flexible piezoelectric cantilever plate integrated gyroscope, *Thin-Walled Structures*, 47(8-9) pp. 836-846
- [9] Nestorovic, T., Marinkovic, D., Chandrashekar, G., Marinkovic, Z., Trajkov, M., 2012, Implementation of a user defined piezoelectric shell element for analysis of active structures, *Finite Elements in Analysis and Design*, 52 pp.11-22
- [10] Nestorović, T., Durrani, N., Trajkov, M., 2012, Experimental model identification and vibration control of a smart cantilever beam using piezoelectric actuators and sensors, *Journal of Electroceramics*, 29(1)
- [11] Oveisi, A., Gudarzi, M., 2013, Nonlinear robust vibration control of a plate integrated with piezoelectric actuator, *International Journal of Mathematical Models and Methods in Applied Sciences*, 7(6) pp. 638-646
- [12] Nestorović T., Köppe H., Gabbert U., 2008: Direct model reference adaptive control (MRAC) design and simulation for the vibration suppression of piezoelectric smart structures, *Communications in Nonlinear Science and Numerical Simulation*, 13(9), 1896-1909
- [13] Géradin, M., 1997, *Mechanical vibrations theory and application to structural dynamics*, second ed., Wiley, Chichester
- [14] Zhou, K., Doyle, J. C., 1997, *Essentials of robust control*, Prentice Hall
- [15] Sivrioglu, S., Tanaka, N., 2002, Acoustic power suppression of a panel structure using  $H_\infty$  output feedback control, *Journal of Sound and Vibration*, 249(5) pp. 885-897
- [16] Chilali, M., Gahinet, P., 1995,  $H_\infty$  design with pole placement constraints:  $H_\infty$  an LMI approach, *IEEE Transactions on Automatic Control*, 41(3) pp. 358-367
- [17] Banjerdpongchai, D., How J. P., 1998, Parametric robust  $H_2$  control design with generalized multipliers via LMI synthesis, *International Journal of Control*, 70(3) pp. 481-503
- [18] Gahinet, P., 1996, Explicit controller formulas for LMI-based  $H_\infty$  synthesis, *Automatica*, 32(7) pp. 1007-1014

- [19] Scherer, C., 1995, Mixed  $H_2/H_\infty$  Control, Trends in Control: A European Perspective, volume of the special contributions to the ECC
- [20] Gudarzi, M., Oveisi, A., Mohammadi, M. M., 2012, Robust active vibration control of a rectangular piezoelectric laminate flexible thin plate: an LMI-based approach, *International Review of Mechanical Engineering*, 6(6) pp. 1217-1227
- [21] Nestorović, T., Trajkov, M., 2013, Optimal actuator and sensor placement based on balanced reduced models, *Mechanical Systems and Signal Processing*, 36(2) pp. 271-289